Congreso de Métodos Numéricos en Ingeniería
12-14 septiembre 2022, Las Palmas de Gran Canaria, España

DYNAMIC SIMULATION OF ONE-SIDED ROCKING MASONRY FAÇADES USING AN ENERGY-CONSISTENT VISCOUS DAMPING MODEL

Georgios Vlachakis[1], Anastasios I. Giouvanidis[1], Anjali Mehrotra[2] and Paulo B. Lourenço[1]

1: Institute for Sustainability and Innovation in Structural Engineering (ISISE)
Department of Civil Engineering, University of Minho
Campus de Azurém, 4800-058 Guimarães, Portugal
e-mail: giorgovlachaki@gmail.com, agiouvanidis@civil.uminho.pt, pbl@civil.uminho.pt
web: http://www.hms.civil.uminho.pt/

2: Department of Materials, Mechanics, Management & Design,
Faculty of Civil Engineering and Geosciences, Delft University of Technology
Buidling 23, Delft, Netherlands
Email: a.a.mehrotra@tudelft.nl
web: https://www.tudelft.nl/

Keywords: one-sided rocking motion, viscous damping, coefficient of restitution, numerical modelling, masonry, out-of-plane

Abstract *Unreinforced masonry façades are specifically vulnerable to seismic actions. Their weak connectivity with adjacent structural members results in their detachment during an earthquake, thus, forming local collapse mechanisms which exhibit one-sided rocking motion. Such mechanisms can accommodate considerable displacements before collapsing/overturning. Hence, their dynamic stability is of great interest. The dynamic response of such collapse mechanisms has been investigated using the classical rocking theory. This is a reliable and fast model that efficiently simulates the dynamic response and energy losses of rocking structures, yet limited to simple structural configurations. As the problem's complexity increases (e.g. degrees of freedom, boundary conditions, and/or material nonlinearities) numerical modelling of such structures has been recently gaining momentum. However, despite the great advances of such numerical modelling techniques, simulation of energy losses still remains challenging. The present work proposes a novel numerical block-based model that efficiently simulates energy losses during one-sided rocking motion. Specifically, an equivalent viscous damping model is adopted and calibrated in a phenomenological fashion after the classical rocking theory. Importantly, the unilateral dashpot formulation of the proposed viscous damping model allows for an accurate replication of the impulsive nature of impacts. Ready-to-use predictive equations are presented, which are also validated against experimental results from literature.*

1. INTRODUCTION

Masonry structures are particularly vulnerable to seismic actions [1]. Frequently, the connections among the different structural members are inadequate and masonry façades tend to detach and form local Out-Of-Plane (OOP) mechanisms that rock on their base [2]. These mechanisms are characterised by a very low force capacity, which makes them prevail among other mechanisms, yet have a non-negligible displacement capacity [3]. As a result, they pose vital dynamic stability, which eventually determines their collapse or safety against earthquakes [4]. In this context, static approaches for assessing this complex behaviour show severe limitations, since inertia dynamic and dissipative phenomena are neglected [5]. In fact, a more accurate estimation of the seismic response of masonry façades may be obtained using dynamic methods of analysis [6].

To this end, classical rocking dynamics have been proposed to assess the seismic response of OOP mechanisms [7]. The rocking motion of a rigid block was described in the seminal work of Housner [8], followed by extensive research and developments on the study of rocking bodies [9]–[13]. Lately, classical rocking dynamics has facilitated many extensions with regard to masonry structural configurations, accommodating the influence of thrusts and floor/roof elements free to move or restrained [14], [15], presence of transversal walls [16], [17] etc. Within this framework, energy losses are assumed to occur when the rocking block impacts its base, and are captured through the Coefficient of Restitution (CoR). More specifically, impact is treated as an instantaneous event. Thus, conservation of angular momentum allows the computation of the CoR based solely on the geometry of the rocking block [8]. Overall, classical rocking dynamics allows a fast and statistically accurate description of the response of simple rocking mechanisms, while energy losses are easily and reliably reproduced [18]–[20]. Nevertheless, the use of classical rocking dynamics becomes more challenging in case the mechanism's complexity increases, e.g. Degrees of Freedom (DoF), boundary conditions (BC), material nonlinearities etc. [21]–[24].

In the meantime, numerical methods in engineering have gained an important momentum the last decades, incorporating developments from different fields into powerful predictive tools. The simulation of masonry structures is easily facilitated in such framework, as the geometrical complexity of masonry's BCs and texture are not restrained by the DoFs of the system, while sophisticated material constitutive laws are usually readily available. The most frequently used block-based numerical models are the Finite Element Method (FEM) [25], the Discrete Element Method (DEM) [26] and the multibody dynamics [27], [28]. Nevertheless, despite their widespread use, such models lack a reliable description of energy losses at impact of rocking bodies [29]–[31]. To this aim, viscous damping models are commonly employed [32], [33], yet without confidence about their energy loss consistency with the classical rocking theory.

The present work aims to bridge the gap of energy losses treatment between the well-established and statistically accurate classical rocking dynamics and the widely used block-based numerical models. This will permit the use of complex numerical rocking models with a reliable representation of the damping phenomena. To this end, a viscous damping model is calibrated to replicate both the manner and extent of energy losses, similarly with the CoR of

classical rocking dynamics. Furthermore, one of the most commonly recurrent OOP mechanisms is studied herein, i.e. the one-sided rocking of façades. This mechanism occurs when a façade detaches from the transversal walls due to their weak connectivity, and thus is free to rock only outwards, while it impacts both with its base and its transversal side walls.

The paper is structures as follows: Section 1 introduces the research framework and presents the objectives of the work. Section 2 describes the dynamics and modelling methods used to analyse the one-sided rocking problem, while Section 3 proceeds with the calibration of a viscous damping dashpot and proposes ready-to-use equations. Section 4 validates the proposed damping model against experimental data of one-sided rocking masonry façades from literature. Finally, Section 5 concludes the work by highlighting the main outcomes and indicating possible future research directions.

2. MODELLING STRATEGIES OF ROCKING STRUCTURES

2.1. Analytical rocking dynamics

Consider a rigid block experiencing planar rocking motion on its base while restrained at its side, as shown in Figure 1 (a). The equation of motion can be written as [8]-[16]:

$$\ddot{\theta} = -p^2 \left[\sin(\alpha - \theta) + \frac{\ddot{u}_g}{g} \cos(\alpha - \theta) \right] \tag{1}$$

where α is the slenderness of the block ($\alpha = \arctan(h/b)$), θ describes the rocking response, $\ddot{u}_g$ denotes the seismic ground acceleration, p is defined as $p = \sqrt{mgR / I_0}$, with m referring to the mass of the block, and I_0 is the rotational moment of inertia with respect to the pivot points. The moment-rotation diagram of the rigid system is indicated by the solid line in Figure 1 (c). Note that Eq. (1) refers to the smooth part of the rocking motion, i.e. when the block pivots, which is identical both for the one-sided rocking (“1s”) studied herein and the classical two-sided rocking (“2s”), as this part of the motion in not affected by the side restrain.

The smooth rocking response is interrupted by non-smooth impacts with its base and side, which are assumed to be instantaneous. Impacts result in loss of energy for the system and are described by the CoR e, which relates the pre-impact and post-impact angular velocities. Furthermore, assuming no bouncing or sliding occurs, the CoR may be computed by applying the conservation of angular momentum (just) before and after the impact. Importantly, this equilibrium yields that the CoR is solely dependent on the geometry of the block, and not a material dependent parameter. In the classical two-sided rocking motion (not restrained at its side), the block impacts only at its base and the CoR reads [8]:

$$e_{2s} = 1 - \frac{3}{2} \sin^2 \alpha \tag{2}$$

In the case of one-sided rocking motion, the block impacts both with the base and the side. Sorrentino et al. [16] pointed out that this results in three consecutive impacts, taking place in

close but distinct time instants. Firstly, the block impacts with the base (point 2 in Figure 1 (a)), followed by an impact at the upper corner of the side (point 3 in Figure 1 (a)) and finally an additional impact with the base (point 1 in Figure 1 (a)). Among them, the first and third impacts are described by Eq. (2), while for the second Sorrentino et al. [16] computed another CoR as:

$$e_{side} = 1 - \frac{3}{2}\cos^2\alpha \tag{3}$$

Therefore, all three impacts during the one-sided rocking motion may be expressed with one lumped CoR as [16]:

$$e_{1s} = e_{2s} \cdot e_{side} \cdot e_{2s} \tag{4}$$

Note that Eq. (3) yields negative values for common cases of slenderness, and thus the lumped one-sided CoR e_{1s} results in a post-impact rocking motion over the same pivot point (point 1 in Figure 1 (a)) but in the opposite direction.

The solution of the analytical problem herein is obtained by solving the differential Eq. (1) interrupted by event-based impacts, using mathematical programming in MATLAB [34].

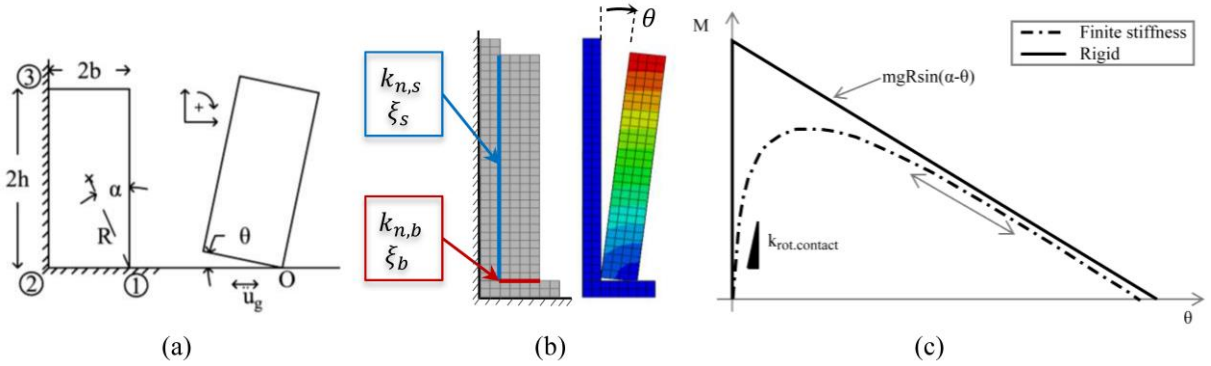

Figure 1. (a) Scheme of the classical rigid block experiencing one-sided rocking motion; (b) Numerical modelling of the one-sided rocking block with finite stiffness; and (c) Moment-rotation diagram of rigid and finite stiffness modelling techniques.

2.2. Numerical modelling of rocking

The simulation of the two parts of rocking motion (i.e. the smooth pivoting and the non-smooth impacts) using block-based numerical methods differs. Firstly, the replication of the smooth part of rocking requires considering the geometrical nonlinearities during the analysis of the problem. Physically, this is related to the stabilising role of the self-weight and its gradual loss upon rotations, while graphically this is depicted by the softening part of the moment-rotation diagram in Figure 1 (c). Furthermore, an essential role in the numerical models is attributed to the contact law adopted to describe the interaction of the different bodies in contact [35]. In general, there are two main strategies to treat contact. On one hand, there are methods that forbid any penetration among the bodies, being a

reasonable physical condition [36]. However, this implies the loss of all the kinetic energy of the colliding nodes and thus the energy losses of the system become numerically mesh-dependent. On the other hand, there exist contact laws that describe interaction of bodies with finite interface stiffness [22], [37], avoiding in this way the introduction of artificial energy losses and thus preserving the system's energy balance [38]. Importantly, the interface stiffness might be used to replicate meso-scale stiffness properties of contacting bodies [39], simulate macro characteristics such as mortar flexibility [19] and degradation [40], or foundation flexibility [41]. Considering the above, this work adopts the latter strategy, with finite interface stiffness acting in the normal direction between the rocking block and the base ($k_{n,b}$) and between the block and the side ($k_{n,s}$), as illustrated in Figure 1 (b). Consequently, the finite stiffness of the system ($k_{rot,contact}$, the moment-rotation curve for which is also shown also in Figure 1 (c)), results in impacts that occur over finite displacement and time, in contrast with the instantaneous behaviour of the analytical model.

To simulate physical energy losses, numerical block-based models usually employ viscous damping formulations, which consist a mathematically convenient way to replicate dissipative phenomena that are not explicitly considered [42]. More specifically, viscous damping models assume that the damping forces are proportional to the velocity of the system, while a variety of alternative formulations are available depending on: i) the DoFs employed, ii) the behaviour of the model during the time-history, and iii) the methods used to calibrate them [43], [44]. In the particular rocking problem examined herein, a stiffness-proportional dashpot formulation acting locally at the contact interfaces composes a convenient way of simulating the instantaneous features of energy losses at impact [29]. Therefore, a unilateral viscous damping is adopted in this work and set to act in parallel with the interface stiffness at the contact interfaces. More specifically, the rocking body interacts with its base with a damping ratio ξ_b and with its side with a damping ratio ξ_s, as shown in Figure 1 (b).

The numerical simulations are herein performed using the FEM software ABAQUS CAE [45], while the solution is advanced using an explicit time-stepping integration scheme. It is worth highlighting that the adopted viscous damping modelling strategy has been validated also in other block-based simulation software [29], including FEM with an implicit scheme and DEM with an explicit scheme. This highlights the universal applicability of the proposed numerical viscous damping model.

3. THE PROPOSED VISCOUS DAMPING MODEL

3.1. Calibration methodology

Viscous damping models are in essence mathematical "artifices", and therefore they need to be tuned to reproduce a desired dissipative behaviour. To this end, this work conducts a phenomenological calibration so that the numerical viscous damping model dissipates energy similarly with the CoR-based rocking dynamics. More specifically, the latter modelling

strategy is assumed as reference, and the former is adjusted to mimic it. Essentially, the objective of the calibration is to find a correlation among the CoR e and the damping ratio ξ, as the former is estimated easily and with confidence, while the latter may be integrated within the numerical block-based models. The workflow of the calibration methodology adopted herein is depicted in Figure 2 and a more detailed description of its key steps follows.

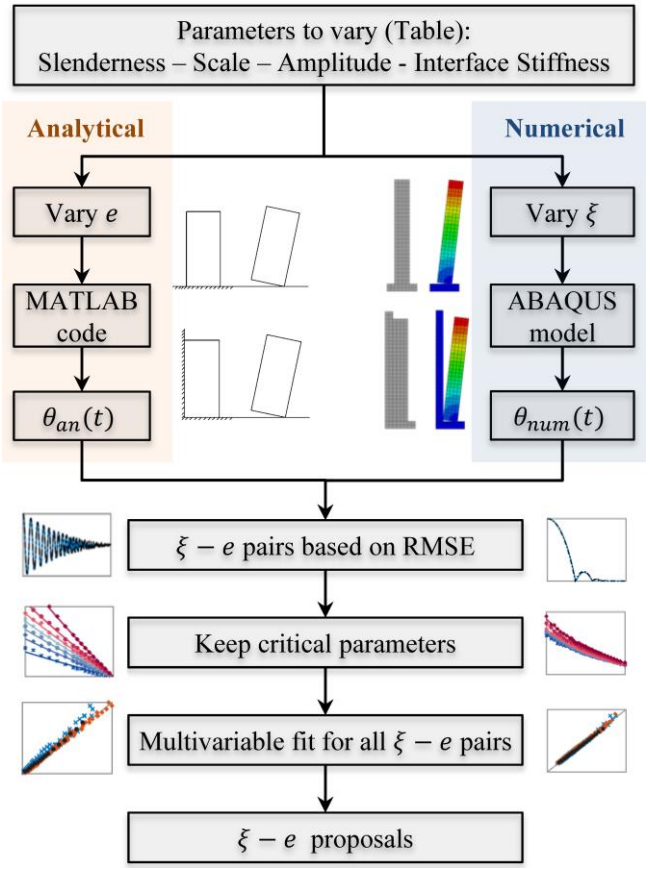

Figure 2. Flowchart of the adopted phenomenological calibration process.

Firstly, all the parameters of the problem are examined in order to identify their influence on the behaviour of the viscous damping model, i.e. i) slenderness h/b, ii) scale R, iii) rocking amplitude θ_0/α, and iv) normal interface stiffness $k_{n,b}$ and $k_{n,s}$. Moreover, the influence of the CoR e is also varied independently of the slenderness of the block, i.e. Eqs. (2-3) are disregarded. This choice allows the viscous damping proposal to be adaptable to any CoR correction suggestions, based either on experimental [16], [19], or theoretical basis [46], [47]. Table 1 collects the range of values that the aforementioned parameters consider in the calibration process, together with their reference value. Afterwards, for each combination of the problem's parameters, numerous free-rocking simulations are performed with both modelling strategies by varying their energy controlling parameter, i.e. the CoR e and the damping ratio ξ. This allows matching the $\xi - e$ pairs that minimise the root mean

square error of the two responses. At this stage, only the essential parameters that influence the viscous damping model are identified and selected, which are found to be the slenderness and the normal interface stiffness at the base [29]. Finally, all the matched $\xi - e$ pairs are employed in a multivariable regression analysis, with the damping ratio being the dependent variable and the CoR together with the slenderness and normal interface stiffness at the base the independent ones. It is worth noting that that since the one-sided rocking problem is characterised by two dependent variables, i.e. the damping ratio at the base ξ_b and the damping ratio at the side ξ_s, the aforementioned problem is overdetermined. Therefore, the proposed calibration methodology is applied in a consecutive way: firstly for the two-sided rocking problem where only ξ_b is included, and afterwards, by presuming the calibrated ξ_b, the problem becomes determined and ξ_s is calibrated in sequence.

Parameter	Range	Reference value
Scale: R [m]	1.4 – 2.8	2.1
Slenderness: h/b [-]	4.0 – 15.0	7.0
Amplitude: θ_0/α [-]	0.3 – 0.8	0.5
Normal interface stiffness at base: $k_{n,b}$ [N/m^3]	$0.5\cdot10^8 - 30\cdot10^8$	$5\cdot10^8$
Normal interface stiffness at side: $k_{n,s}$ [N/m^3]	$0.5\cdot10^8 - 30\cdot10^8$	$5\cdot10^8$

Table 1. Independent parameters considered for the calibration process (Figure 2).

3.2. Proposed viscous damping model

The application of the aforementioned calibration methodology results in two predictive $\xi - e$ equations, one for the damping ratio acting at the base ξ_b and one for the damping ratio acting at the side ξ_s:

$$\xi_b = -0.000292 \cdot \left(\frac{h}{b}\right)^{0.935} \cdot k_{n,b}{}^{0.343} \cdot \ln e_{2s} \tag{5}$$

$$\xi_s = -0.0807 \cdot \left(\frac{h}{b}\right)^{0.2548} \cdot k_{n,b}{}^{-0.1283} \cdot \ln \left|e_{side}\right| \tag{6}$$

Note that Eqs. (5-6) have been generated after more than a thousand numerical simulations and are characterised by a coefficient of determination $R^2 = 0.978$ and $R^2 = 0.994$, respectively, indicating a noteworthy predictive capability.

An illustrative example of the performance of the calibration methodology and Eqs. (5-6) is shown in Figure 3. The comparison examines the one-sided free rocking response of a block with height $2h = 4.2$ m and width $2b = 0.6$ m, analysed using both the analytical rocking dynamics outlined in Section 2.1 and the numerical model described in Section 2.2. The analytical model includes a CoR acting at the base $e_{2s} = 0.97$ (Eq. (2)) and a CoR acting

at the side $e_{side} = -0.47$ (Eq. (3)). The numerical model assumes equal normal interface at the base and side $k_{n,b} = k_{n,s} = 5 \cdot 10^8$ N/m^3, while the damping ratios of the base and side are computed using Eqs. (5-6), accordingly as $\xi_b = 5.3$ % and $\xi_s = 0.74$ %. Figure 3 (a) depicts the rocking angle of the response, while Figure 3 (b) compares the corresponding (total) energy content of the models (i.e. kinetic and potential). Overall, the two models show a very good agreement, despite being fundamentally different. More specifically, the proposed viscous damping model appears to dissipate with a step-like manner at impacts alike the CoR-based model, while the amount of dissipated energy matches well owing to the calibration procedure.

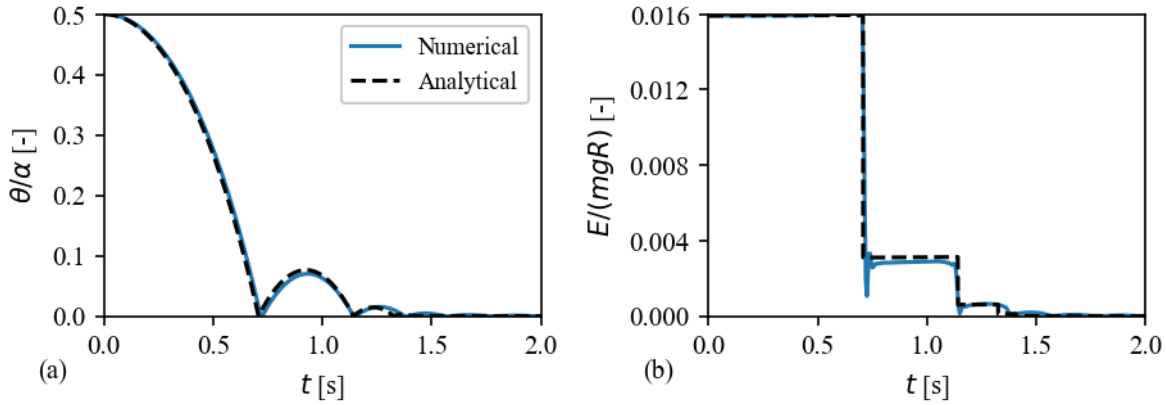

Figure 3. Behaviour of the viscous damping model. Comparison with the analytical model, in terms of variation of the (a) rocking angle and (b) total energy content over time. Details of the examined structure: $2h = 4.2$ [m], $2b = 0.6$ [m], $e_{2s} = 0.97$, $e_{side} = -0.47$, $k_{n,b} = k_{n,s} = 5 \cdot 10^8$ [N/m^3], $\xi_b = 5.3$ [%] and $\xi_s = 0.74$ [%].

4. PERFORMANCE OF THE VISCOUS DAMPING MODEL

This section assesses the performance of the proposed numerical viscous damping model. While its calibration has been based on the analytical rocking model, its robustness is tested using actual experimental results. To this end, the experimental campaign reported in [16] is used, where a variety of masonry walls were tested under one-sided free rocking vibrations. Details regarding the specimens' characteristics can be found in Table 2, while the interested reader is referred to the original experimental work of [16] for further details. Given the fact that the proposed model has been calibrated independently of Eqs. (2-4), the experimentally measured CoR e_{1s} can be inserted in Eqs. (5-6) to get the damping ratio of the viscous damping model and obtain a better replication of the experimental results.

Reference code	H [m]	α_{exp} [rad]	$e_{1s,exp}$ [-]	ξ_b [%]	ξ_s [%]
brick, h80, cd12, t01	0.8	0.1184	-0.328	4.35	1.15
brick, h82, cd06, t03	0.82	0.1157	-0.441	4.24	0.84
brick, h136, cd06, t01	1.36	0.0420	-0.458	1.44	1.09
brick, h163, cd06, t01	1.63	0.0371	-0.273	1.26	1.87
tuff, h128, cd12, t02	1.28	0.0699	-0.403	2.48	1.10
tuff, h163, cd12, t02	1.63	0.0546	-0.309	1.90	1.52
Note: Reference code: material, height (cm), contact depth of sidewalls, test number.					

Table 2. Details of the examined specimens and tests [16]

Figure 3 collects the response histories of all the examined cases reported in Table 2. More specifically, it compares the experimental outcomes provided by [16] against the results obtained with the numerical model. In general, it appears that the proposed numerical viscous damping model presents a very good estimation of the experimental response of all the masonry walls. Some rather small differences may be observed among them, yet within an acceptable level considering the experimental uncertainties of such campaigns. Nevertheless, the dissipative phenomena are still very well captured by the numerical viscous damping model: significant amount of energy is lost at impact, resulting in the damping out of the oscillation after two or three impacts.

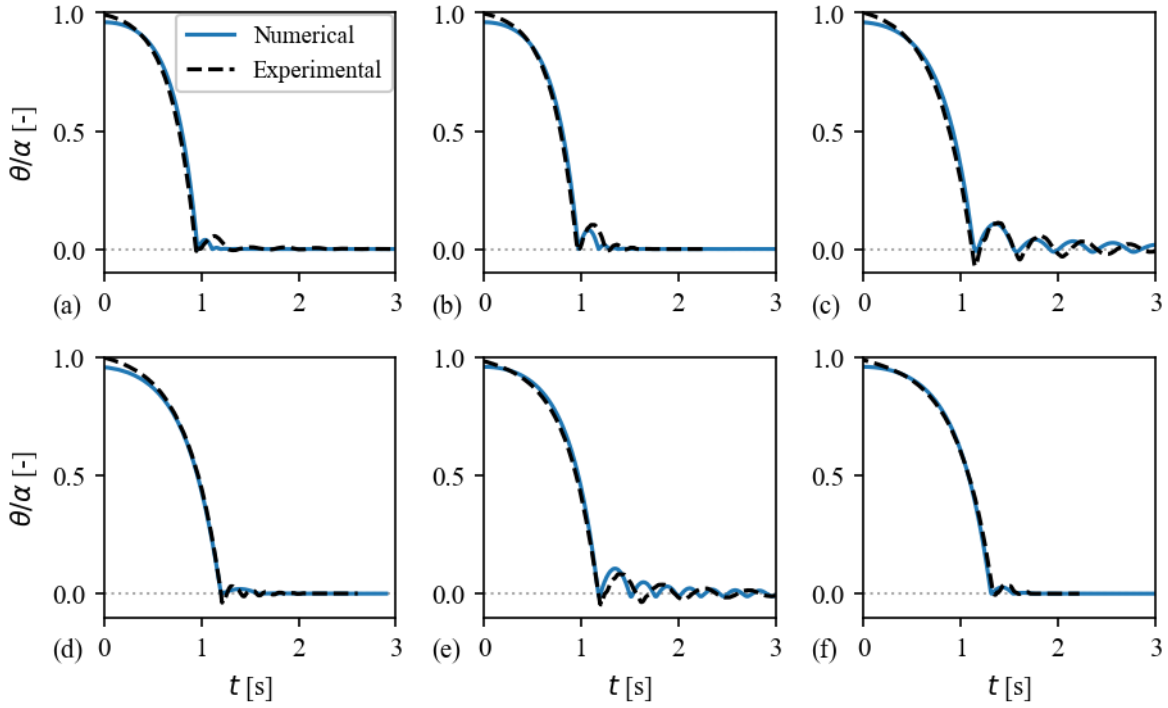

Figure 4. Free-rocking response of the proposed numerical viscous damping model compared with ethe experimental response reported in [16]: (a) brick, h80, cd12, t01, (b) brick, h82, cd06, t03, (c) brick, h136, cd06, t01, (d) brick, h163, cd06, t01, (e) tuff, h128, cd12, t02, and (f) tuff, h163, cd12, t02 (Table 2).

5. CONCLUSIONS

This work presents a numerical strategy for modelling the dynamic response of one-sided rocking mechanisms with particular focus on the energy losses. More specifically, it proposes a viscous damping model that dissipates similarly with the CoR-based analytical rocking dynamics. This is achieved by following a phenomenological calibration methodology, where the analytical model is assumed as reference and the viscous damping model is tuned to mimic the former. After over a thousand of numerical simulations, predictive ready-to-use equations are provided that respect energy consistency of the two fundamentally different models. Importantly, the proposed stiffness-proportional unilateral dashpot model results in impulsive energy losses similarly to that of the CoR-based model. Finally, the performance of the proposed model is evaluated against experimental results available in literature, showing very good predictive capabilities.

In conclusion, the current paper presents a reliable and consistent way to model the damping phenomena of rocking structures when using numerical block-based models. This allows the simulation of even more complex structures, with many DoFs, varying BCs or material nonlinearities with ease, overcoming difficulties faced by the analytical rocking dynamics. Moreover, the proposed viscous damping model is universal and adaptable, as it can be used with any block-based numerical method and with any experimental or theoretical corrections on the adopted CoR.

REFERENCES

[1] M. Bruneau, "State-of-the-art report on seismic performance of unreinforced masonry buildings," *J. Struct. Eng.*, vol. 120, no. 1, pp. 230–251, 1994.

[2] G. Vlachakis, E. Vlachaki, and P. B. Lourenço, "Learning from failure: Damage and Failure of Masonry Structures, after the 2017 Lesvos Earthquake (Greece)," *Eng. Fail. Anal.*, vol. 117, 2020.

[3] G. de Felice, S. De Santis, P. B. Lourenço, and N. Mendes, "Methods and Challenges for the Seismic Assessment of Historic Masonry Structures," *Int. J. Archit. Herit.*, vol. 11, no. 1, pp. 143–160, 2017.

[4] A. Mauro, G. de Felice, and M. J. DeJong, "The relative dynamic resilience of masonry collapse mechanisms," *Eng. Struct.*, vol. 85, pp. 182–194, 2015.

[5] M. Godio and K. Beyer, "Evaluation of force-based and displacement-based out-of-plane seismic assessment methods for unreinforced masonry walls through refined model simulations," *Earthq. Eng. Struct. Dyn.*, vol. 48, no. 4, pp. 454–475, 2019.

[6] N. Mendes *et al.*, "Methods and Approaches for Blind Test Predictions of Out-of-Plane Behavior of Masonry Walls: A Numerical Comparative Study," *Int. J. Archit. Herit.*, vol. 11, no. 1, pp. 59–71, 2017.

[7] C. Casapulla, L. Giresini, and P. B. Lourenço, "Rocking and Kinematic Approaches for Rigid Block Analysis of Masonry Walls : State of the Art and Recent Developments," *Buildings*, vol. 7, no. 3, 2017.

[8] G. Housner, "The behavior of inverted pendulum structures during earthquakes," *Bull. Seismol. Soc. Am.*, vol. 53, no. 2, pp. 403–417, 1963.

[9] A. I. Giouvanidis, E. G. Dimitrakopoulos, and P. B. Lourenço, "Chattering: An overlooked peculiarity of rocking motion," *Nonlinear Dyn.*, 2022.
[10] A. I. Giouvanidis and E. G. Dimitrakopoulos, "Rocking amplification and strong-motion duration," *Earthq. Eng. Struct. Dyn.*, vol. 47, no. 10, pp. 2094–2116, 2018.
[11] A. I. Giouvanidis and Y. Dong, "Seismic loss and resilience assessment of single - column rocking bridges," *Bull. Earthq. Eng.*, 2020.
[12] N. Reggiani Manzo and M. F. Vassiliou, "Displacement-based analysis and design of rocking structures," *Earthq. Eng. Struct. Dyn.*, vol. 48, no. 14, pp. 1613–1629, 2019.
[13] N. R. Manzo and M. F. Vassiliou, "Simplified analysis of bilinear elastic systems exhibiting negative stiffness behavior," *Earthq. Eng. Struct. Dyn.*, 2020.
[14] L. Giresini, M. Fragiacomo, and P. B. Lourenço, "Comparison between rocking analysis and kinematic analysis for the dynamic out-of-plane behavior of masonry walls," *Earthq. Eng. Struct. Dyn.*, vol. 44, no. 13, pp. 2359–2376, 2015.
[15] O. AlShawa, D. Liberatore, and L. Sorrentino, "Dynamic One-Sided Out-Of-Plane Behavior of Unreinforced-Masonry Wall Restrained by Elasto-Plastic Tie-Rods," *Int. J. Archit. Herit.*, vol. 13, no. 3, pp. 340–357, 2019.
[16] L. Sorrentino, O. AlShawa, and L. D. Decanini, "The relevance of energy damping in unreinforced masonry rocking mechanisms. Experimental and analytic investigations," *Bull. Earthq. Eng.*, vol. 9, no. 5, pp. 1617–1642, 2011.
[17] O. Al Shawa, G. De Felice, A. Mauro, and L. Sorrentino, "Out-of-plane seismic behaviour of rocking masonry walls," *Earthq. Eng. Struct. Dyn.*, vol. 41, no. 5, pp. 949–968, 2012.
[18] P. R. Lipscombe and S. Pellegrino, "Free Rocking of Prismatic Blocks," *J. Eng. Mech.*, vol. 119, no. 7, pp. 1387–1410, 1993.
[19] A. A. Costa, A. Arêde, A. Penna, and A. Costa, "Free rocking response of a regular stone masonry wall with equivalent block approach: experimental and analytical evaluation," *Earthq. Eng. Struct. Dyn.*, vol. 42, no. 15, pp. 2297–2319, 2013.
[20] J. A. Bachmann, M. Strand, M. F. Vassiliou, M. Broccardo, and B. Stojadinović, "Is rocking motion predictable?," *Earthq. Eng. Struct. Dyn.*, vol. 47, no. 2, pp. 535–552, 2018.
[21] A. I. Giouvanidis and E. G. Dimitrakopoulos, "Seismic Performance of Rocking Frames with Flag-Shaped Hysteretic Behavior," *J. Eng. Mech.*, vol. 143, no. 5, 2017.
[22] A. Mehrotra and M. J. Dejong, "A methodology to account for interface flexibility and crushing effects in multi-block masonry collapse mechanisms," *Meccanica*, vol. 55, pp. 1237–1261, 2020.
[23] E. G. Dimitrakopoulos and A. I. Giouvanidis, "Seismic response analysis of the planar rocking frame," *J. Eng. Mech.*, vol. 141, no. 7, p. 04015003, 2015.
[24] M. F. Vassiliou, "Seismic response of a wobbling 3D frame," *Earthq. Eng. Struct. Dyn.*, vol. 47, no. 5, pp. 1212–1228, 2018.
[25] A. M. D'Altri *et al.*, "Modeling Strategies for the Computational Analysis of Unreinforced Masonry Structures: Review and Classification," *Arch. Comput. Methods Eng.*, vol. 27, pp. 1153–1185, 2019.
[26] J. V Lemos, "Discrete Element Modeling of the Seismic Behavior," *Buildings*, vol. 9,

no. 2, 2019.
[27] A. I. Giouvanidis and E. G. Dimitrakopoulos, "Nonsmooth dynamic analysis of sticking impacts in rocking structures," *Bull. Earthq. Eng.*, vol. 15, no. 5, pp. 2273–2304, 2017.
[28] F. Portioli and L. Cascini, "Contact Dynamics of Masonry Block Structures Using Mathematical Programming," *J. Earthq. Eng.*, vol. 22, no. 1, 2018.
[29] G. Vlachakis, A. I. Giouvanidis, A. Mehrotra, and P. B. Lourenço, "Numerical block-based simulation of rocking structures using a novel universal viscous damping model," *J. Eng. Mech.*, vol. 147, no. 11, 2021.
[30] F. Galvez, L. Sorrentino, D. Y. Dizhur, and J. M. Ingham, "Seismic rocking simulation of unreinforced masonry parapets and façades using the discrete element method," *Earthq. Eng. Struct. Dyn.*, 2022.
[31] M. F. Vassiliou *et al.*, "Shake table testing of a rocking podium : Results of a blind prediction contest," *Earthq. Eng. Struct. Dyn.*, vol. 50, no. 4, pp. 1043–1062, 2021.
[32] J. V. Lemos and A. Campos Costa, "Simulation of Shake Table Tests on Out-of-Plane Masonry Buildings. Part (V): Discrete Element Approach," *Int. J. Archit. Herit.*, vol. 11, no. 1, pp. 117–124, 2017.
[33] D. Malomo, A. Mehrotra, and M. J. Dejong, "Distinct element modeling of the dynamic response of a rocking podium tested on a shake table," *Earthq. Eng. Struct. Dyn.*, vol. 50, no. 5, pp. 1469–1475, 2021.
[34] MathWorks, *MATLAB: The Language of Technical Computing.* Natick, MA: MathWorks, Inc., 1992.
[35] P. Flores, "Contact mechanics for dynamical systems : a comprehensive review," *Multibody Syst. Dyn.*, vol. 54, pp. 127–177, 2021.
[36] M. Jean, "The non-smooth contact dynamics method," *Comput. Methods Appl. Mech. Eng.*, vol. 177, no. 3–4, pp. 235–257, 1999.
[37] A. Mehrotra and M. J. DeJong, "The influence of interface geometry, stiffness, and crushing on the dynamic response of masonry collapse mechanisms," *Earthq. Eng. Struct. Dyn.*, vol. 47, no. 13, pp. 2661–2681, 2018.
[38] J. V Lemos, "Discrete Element Modeling of Masonry Structures," *Int. J. Archit. Herit.*, vol. 1, no. 2, pp. 190–213, 2007.
[39] P. B. Lourenço, D. V. Oliveira, P. Roca, and A. Orduña, "Dry joint stone masonry walls subjected to in-plane combined loading," *J. Struct. Eng.*, vol. 131, no. 11, pp. 1665–1673, 2005.
[40] M. C. Griffith, N. Lam, J. L. Wilson, and K. Doherty, "Experimental Investigation of Unreinforced Brick Masonry Walls in Flexure," *J. Struct. Eng.*, vol. 130, no. 3, 2004.
[41] P. D. Spanos, A. Di Matteo, A. Pirrotta, and M. Di Paola, "Rocking of rigid block on nonlinear flexible foundation," *Int. J. Non. Linear. Mech.*, vol. 94, pp. 362–374, 2017.
[42] F. A. Charney, "Unintended consequences of modeling damping in structures," *J. Struct. Eng.*, vol. 134, no. 4, pp. 581–592, 2008.
[43] J. F. Hall, "Problems encountered from the use (or misuse) of Rayleigh damping," *Earthq. Eng. Struct. Dyn.*, vol. 35, no. 5, pp. 525–545, 2006.
[44] U. Tomassetti, F. Graziotti, L. Sorrentino, and A. Penna, "Modelling rocking response

via equivalent viscous damping," *Earthq. Eng. Struct. Dyn.*, vol. 48, no. 11, pp. 1277–1296, 2019.

[45] Simulia, *Abaqus 6.12 documentation*. Rhode Island, US: Dassault Systèmes Simulia, 2012.

[46] T. Ther and L. P. Kollar, "Refinement of Housner's model on rocking blocks," *Bull. Earthq. Eng.*, vol. 15, pp. 2305–2319, 2017.

[47] D. Kalliontzis, S. Sritharan, and A. Schultz, "Improved Coefficient of Restitution Estimation for Free Rocking Members," *J. Struct. Eng.*, pp. 1–7, 2016.